10th International Conference on Fracture Mechanics of Concrete and Concrete Structures
FraMCoS-X
G. Pijaudier-Cabot, P. Grassl and C. La Borderie (Eds)
https://doi.org/10.21012/FC10.233287

MODELLING THE STOCHASTIC TENSILE BEHAVIOR AND MULTIPLE CRACKING OF STRAIN-HARDENING CEMENTITIOUS COMPOSITES (SHCCS)

JUNXIA LI, JIAN WENG AND EN-HUA YANG

Nanyang Technological University
50 Nanyang Avenue, Singapore 639798
e-mail: jxli@ntu.edu.sg
e-mail: jweng004@e.ntu.edu.sg
e-mail: ehyang@ntu.edu.sg

Key words: Stochastic; Strain-hardening cementitious composites; SHCC; Tensile behaviour; Variability

Abstract: Strain-hardening cementitious composites (SHCCs) have gained the growing application in the infrastructures with exhibiting superior tensile behavior by the formation of the fine multiple cracking. The micromechanics-based method is in the light of governing mechanisms of the multiple cracking by considering the interaction between the fiber, the matrix and the fiber/matrix interface, and thus has the ability to model the tensile behavior of SHCCs, crack characteristics in particular. However, the variability of the tensile behavior (*i.e.*, the tensile strain capacity, the tensile strength, the multiple cracking sequence, the crack spacing, and the crack width) are observed due to the heterogeneity nature of fiber-reinforced cementitious composites, which cannot be completely considered in the existing models. The heterogeneity may originate from variation of properties of ingredients such as inconsistent fiber diameter and fiber strength, processing (variation of flaw size and distribution and non-uniform fiber distribution), and curing. **In this paper, a micromechanics-based stochastic model to capture the variability of SHCC multiple cracking and tensile behavior is developed.** The modelling approach is based on the multi-scale linking from micro-mechanical properties to macro tensile properties through fiber-bridging properties and matrix properties at the meso-level. The pivotal idea is to treat all the micro-mechanical parameters as stochastic variables at the micro-level, in addition, the multiple cracking criteria was firstly introduced in the model to capture the variability of the tensile behavior. Since this analytical model was implemented in a numerical way, it would become a flexible and easy-to-use software package for the engineering application in the future. The capability of the proposed model was confirmed compared with experimental results. Using the newly developed model, parametric studies were conducted to point out that σ_{fu}, V_f, and τ_0 are the most critical parameters to affect the tensile strain capacity of SHCCs.

1 INTRODUCTION

Strain-hardening cementitious composites (SHCCs) are characterized by the strain-hardening behavior and fine multiple cracking in tension [1-3]. However, heterogeneous nature of cement-based material is inevitable. Heterogeneity may originate from variation of properties of ingredients such as inconsistent fiber diameter and fiber strength, processing (variation of flaw size and distribution and non-uniform fiber distribution [4]), and curing. It results in the variability of the composite behavior of SHCCs, including the variability

of the tensile stress-stain relationship, the multiple cracking sequence, crack spacing distribution, and crack width distribution as Fig. 1.

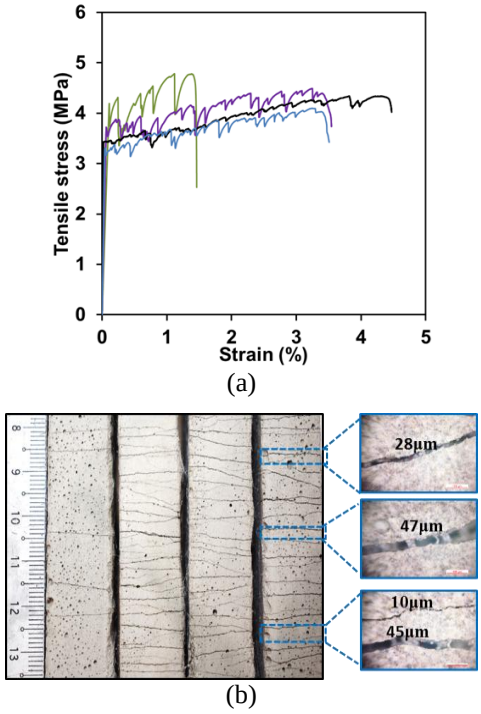

Figure 1: Tensile behavior of SHCC specimens from the same batch, showing a wide distribution of (a) tensile stress-strain relations; (b) crack spacing and crack width

Different models to capture the tensile behavior of SHCCs have been developed with finite element method (FEM) [5-7], discrete element method (DEM) [8-10], and micromechanics-based method [11-15]. FEM- and DEM-based models are able to capture the tensile stress-strain relation. However, they cannot capture all the crack characteristics with covering the underlying mechanism of the multiple cracking process. The mechanism behind the multiple cracking process is the variability of the microstructures [16]. The micromechanics-based models are in the light of the governing mechanisms of multiple cracking by considering the interaction between fiber, matrix and fiber/matrix interface, and thus has the ability to model the tensile behavior of SHCCs, crack characteristics in particular.

However, the existing micromechanics-based models cannot capture all the variability of the composite behavior due to the neglect of some microstructural properties. For example, Lu and Leung [17] developed a model to simulate sequential formation of multiple cracks by considering the non-uniform distribution of the matrix strength. Still, the variability of the tensile stress-strain relation, crack spacing distribution and crack width distribution cannot be modelled because the fiber-bridging properties of each crack plane were assumed to be the same. Kabele [18] developed a stochastic model of multiple cracking process by taking the variability of the matrix strength and the fiber-bridging properties into account, in which, the flaw size and the fiber volume were treated as random variables. While the steady-state cracking criterion of SHCCs was not employed for the determination of multiple cracking and the cracking sequence was simply determined by the descending order of the flaw size.

In this paper, the variability of SHCCs tensile behavior is modelled using the micromechanics-based method with fully comply the underlying mechanisms of the multiple cracking (e.g., steady-state crack propagation). Hence, the mechanism of the multiple cracking process is clarified first, followed by the modelling approach and implementation process. The key point here is to treat all the micro-mechanical parameters representing the fiber, matrix, and fiber/matrix interface properties as random variables. The model is then validated by comparing the simulated results with experiments. Lastly, parametric study is carried out to reveal the significance of each micro-mechanical parameter on the strain capacity of SHCCs.

2 MECHANISM OF THE MULTIPLE CRACKING PROCESS

The tensile strain-hardening of SHCCs is a result of formation of multiple steady-state cracks which requires a) the composite cracking strength σ_c to be less than the maximum fiber-bridging strength σ_0 (Eqn. 1),

and b) the matrix toughness J_{tip} must not exceed the maximum complementary energy $J_b^{'}$ of fiber-bridging (Eqn. 2) [13, 19-24].

$$\sigma_0 \geq \sigma_c \quad (1)$$

$$J_b^{'} \geq J_{tip} \quad (2)$$

The maximum complementary energy $J_b^{'}$ of fiber-bridging can be calculated from the fiber-bridging $\sigma_B(\delta)$ curve [25]. Fulfilment of Eqn. 1 allows the initiation of cracks, while satisfactory of Eqn. 2 ensures cracks propagate in the steady-state mode.

Due to the material heterogeneity, fiber-bridging properties and matrix properties in SHCCs may vary from location to location. As a result, the formation of multiple cracks is sequential and terminates randomly with different level of saturation of multiple cracks. Furthermore, the crack width among different cracks and the spacing between the adjacent two cracks may also be different. Fig. 2 illustrates the multiple cracking process of a SHCC specimen in tension.

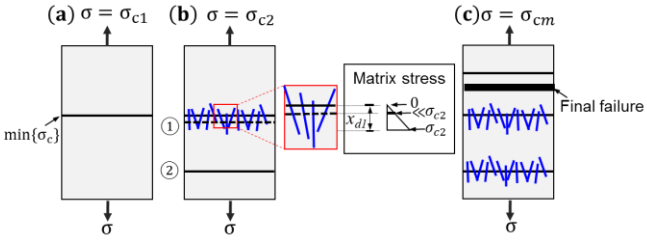

Figure 2: Illustration of multiple cracking sequence

As can be seen, the first crack initiates at the location with the lowest composite cracking strength, i.e., $\min\{\sigma_c\} = \sigma_{c1}$ (Fig. 2a). Satisfaction of both Eqns. 1 and 2 at this crack plane is necessary to ensure steady-state crack propagation prevails in tension and to prevent damage localization. The corresponding stress and strain of the specimen at its first cracking defines the starting point of the tensile strain-hardening [3, 13].

With increased stress to σ_{c2}, the second crack occurs at the location outside the critical transfer distance of the first crack (i.e., x_{d1} in Fig. 2b) with the composite matrix strength of σ_{c2} (e.g., section ② in Fig. 2b). This is because the matrix at the first crack plane becomes stress free and the stress gradually transfers back to the matrix through the fiber/matrix interface friction and the fiber/matrix interface pulley force due to fiber inclination, and up to σ_{c2} at x_{d1}. Thus, the matrix stress within x_{d1} (e.g., section ① in Fig. 2b) is less than σ_{c2} which cannot initiate the next crack in this region. That is to say, the composite cracking strength σ_{ci} and the stress transfer distance x_{di} jointly determine the occurrence of the multiple cracking in the specimen. Again, satisfaction of both Eqns. 1 and 2 at the second crack plane is necessary to ensure steady-state crack propagation prevails in tension and to prevent damage localization. In addition, it is worth noting that value of x_d of different crack plane can be different because x_d is largely governed by the fiber and fiber-matrix interface properties (and so are the fiber-bridging properties) of individual crack plane.

With the continuous increase of loading, more steady-state cracks form in sequential until the applied stress reaches the lowest bridging strength among all crack planes (i.e., $\min\{\sigma_{0i}\}$) or Eqns. 1 or 2 is not satisfied at the m^{th} crack, which defines the termination of multiple cracking and tensile strain-hardening (Fig. 2c), as well as the final failure.

3 MULTISCALE LINKING MODELLING APPROACH

Fig. 3 presents the multiscale linking approach for the development of the micromechanics-based stochastic model to capture the variability of tensile behavior of SHCCs in the current study. At the micro-level, three microstructural phases in terms of the fiber, matrix and fiber/matrix interface properties can be characterized by the single fiber behavior, the existing flaw distribution and the single fiber pullout behavior, respectively. A set of thirteen micro-mechanical parameters is used to describe the three phases [16], which are considered as random variables to capture their heterogeneity herein. With the specified

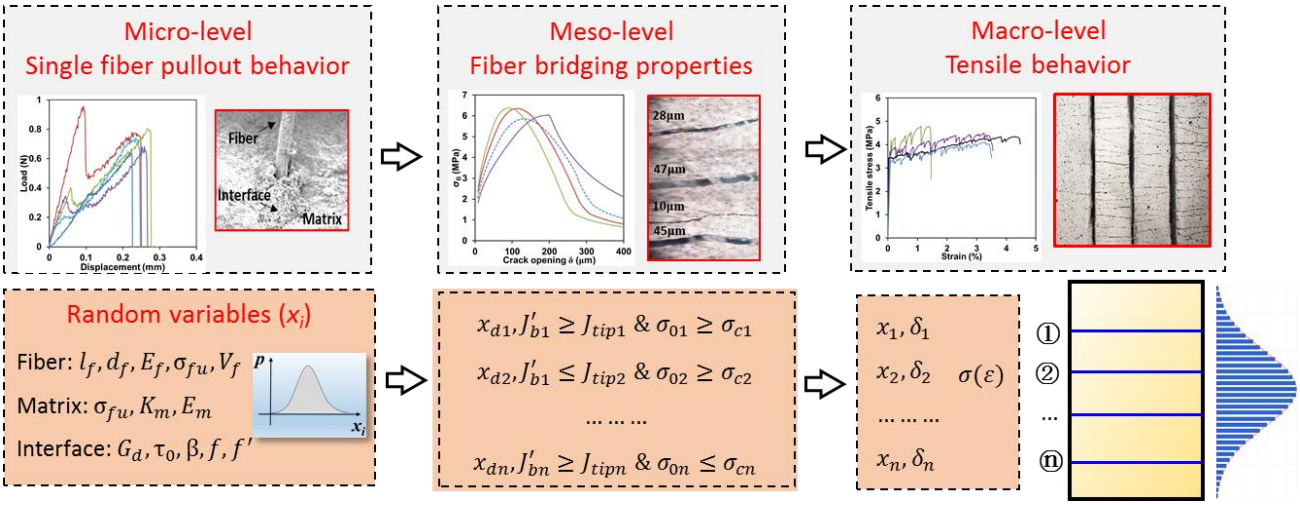

Figure 3: Multiscale linking approach for modelling the variability of SHCC tensile behavior

micro-mechanical parameters, the variability of fiber-bridging properties and matrix cracking properties, which govern the multiple cracking and strain-hardening performance of SHCCs, can be determined at the meso-level. As a consequence, the variability of the tensile behavior of SHCCs, *i.e.*, tensile stress-strain curve, cracking sequence, crack width distribution and crack spacing distribution can be modelled at the macro-level.

In the current study, this multiple cracking process is modelled numerically. Fig. 4 depicts the flow chart of the proposed micromechanics-based method of modelling the variability of SHCC tensile behavior. In the first part, a SHCC specimen is defined with specifying the number of equal sections n over the gauge length L. The n equal sections define potential crack planes. Monte Carlo simulation is used to generate the values of micro-mechanical parameters for each crack plane according to the given statistical distribution of each micro-mechanical parameter along the loading direction. The generated micro-mechanical parameters in each cracking plane are used as a set of inputs to calculate the fiber-bridging $\sigma_B(\delta)$ curve (*e.g.*, σ_0 and J'_b), composite cracking strength σ_c, and matrix toughness J_{tip} of that particular crack plane.

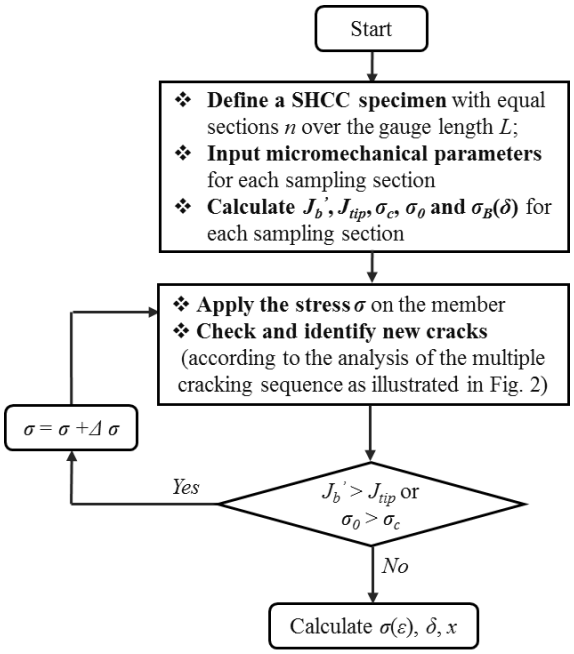

Figure 4: Flow chart of the proposed model

Then, the SHCC specimen is numerically loaded under stress control. Formation of cracks is checked and identified at each load step according to the analysis of the multiple cracking sequence as illustrated in Fig. 2. At each load step j, x_{di} for each crack plane can be calculated and corresponding crack opening δ_i of each crack plane can be derived from the fiber-bridging constitutive law $\sigma_B(\delta)$ by equalling σ_{Bi} to σ_j (*i.e.*, the overall stress applied on the specimen in step j). It is noted

that this approximation ($\sigma_{Bi} \approx \sigma_i$) results in the neglect of the stress fluctuation as Fig. 1, due to force equilibrium between the cracked section and the adjacent uncracked composite section. Consequently, the multiple cracking sequence, crack width, crack spacing can be attained from the cracking process simulation.

Finally, the simulation terminates once the final failure occurs (*e.g.*, the applied stress reaches the lowest bridging strength among all crack planes $\min\{\sigma_{0i}\}$ or Eqns. 1 or 2 is not satisfied at the m^{th} crack) and the $\sigma(\varepsilon)$ curve can be output. The stress σ is the applied stress. The strain capacity ε can be calculated by summing up the elastic strain and opening of each crack δ_i as

$$\varepsilon = \sigma_j/E_c + (\delta_1 + \delta_2 + \ldots + \delta_m)/L \quad (3)$$

where j is the applied loading step, L is the gauge length of the SHCC specimen, and m is the number of cracks within the gauge length, which can be known from modelling the multiple cracking process.

4 MODELLING VALIDATION

4.1 Experimental design

The proposed micromechanics-based model is first validated by comparing the simulated results with experimental data. A typical SHCC mix (M45) is selected for model validation and the mix design is summarized in Table 1 [25, 26]. The ingredients of M45 include Type I ordinary Portland cement, ASTM Class F fly ash, micro silica sand with a mean size of 110 μm, water, superplasticizer, and PVA fibers. The fibers have the diameter of 39 μm, the length of 12 mm, the in-situ tensile strength of 900 MPa and Young's modulus of 24 GPa. The surface of PVA fibers was coated with hydrophobic oiling agent of 1.2% by weight to control the interface properties of the fiber and matrix.

Table 1: Mix composition of SHCC M45

Cement	Water	Sand	Fly ash	Fiber	SP
1.0	0.53	0.8	1.2	2%	0.03

Note: All numbers are weight ratios except for fiber volume

To evaluate the tensile behavior, 4 coupon specimens 300 × 75 × 12 mm^3 were employed to conduct the direct tensile test. Aluminium plates were glued both sides at the ends of coupon specimens to facilitate gripping. Two external linear variable displacement transducers were attached to the specimen with a gauge length of approximately 150 mm to measure the specimen deformation. The coupons were tested under uniaxial tension with fixed-fixed end grip. All specimens were cured in air (28˚C and 65% RH) for 28 days. Direct tensile tests were carried out under displacement controlled by means of a 50 kN universal testing machine at a loading speed of 0.3 mm/min.

4.2 Simulation procedure

The simulation procedure follows the steps as Fig. 4. Firstly, the modelled specimen is defined to have a length of 150 mm, the same as the gauge length in the direct tensile test. Two discretization fineness, *i.e.*, 150 equal sections (1 mm for each section) and 1000 equal sections (0.15 mm for each section), were used. All micro-mechanical parameters are considered as random variables and Table 2 summarizes the distribution and values of micro-mechanical parameters used in the model calculation. The fiber length L_f and the fiber diameter d_f follow normal distribution and the values are measured directly. The fiber modulus E_f, the fiber strength σ_{fu}, the fiber/matrix interface properties G_d, τ_0, β, the matrix modulus E_m and the matrix toughness K_m are experimentally determined [27] and are assumed to follow normal distribution in the current study. The fiber volume V_f is assumed as normal distribution. A coefficient is introduced to describe the degree of dispersion of fiber as fiber clumps and bundles were often observed in experiments [28]. The snubbing coefficient f and the fiber strength reduction coefficient f' follow uniform distribution and

Table 2: Micro-mechanical parameters of the mix

Micro-mechanical parameters		Distribution	Value	Reference
Fiber	E_f (GPa)	Normal	Mean = 24, STD = 6	[27]
	L_f (mm)	Normal	Mean = 12, STD = 1.2	Measured
	d_f (μm)	Normal	Mean = 39, STD = 3.9	Measured
	σ_{fu} (MPa)	Normal	Mean = 900, STD = 30	[27]
	V_f (%)	Normal	Mean = 2, STD = 0.1	Assumed
	λ	Uniform	0.85	Assumed
Interface	G_d (J/m^2)	Normal	Mean = 1.08, STD = 0.8	[27]
	τ_0 (MPa)	Normal	Mean = 1.31, STD = 0.1	[27]
	β	Normal	Mean = 0.53, STD = 0.3	[27]
	f'	Uniform	0.33	[16, 29]
	f	Uniform	0.2	[16, 29]
Matrix	E_m (GPa)	Normal	Mean = 20, STD = 2	[27]
	σ_{mu} (MPa)	Weibull	λ = 4, k = 20.4	[17]
	K_m (MPa·m$^{1/2}$)	Normal	Mean = 0.59, STD = 0.06	[27]

are determined by single fiber in-situ strength test [16, 29]. The matrix strength σ_{mu} is assumed as Weibull distribution which is generally used [17], and the parameter of the distribution is attained by fitting the experimental data.

10 simulated direct tensile tests are carried out. For each simulated test, Monte Carlo simulation is used to generate the values of micro-mechanical parameters in each crack plane according to the given statistical distribution of each micro-mechanical parameter along the loading direction. The generated micro-mechanical parameters in each cracking plane are used as a set of inputs to calculate the composite behavior under direct tension as described in Section 3.

4.3 Results and discussion

Fig. 5 plots the representative tensile stress-stain curves of SHCC M45 obtained from experiments and numerical simulations. Table 3 further summarizes the average values and standard deviations of tensile properties of SHCC M45 determined through experiments and numerical simulations. It can be seen from the experimental results that tensile properties (*e.g.*, tensile strain capacity) of SHCC M45 shows variability due to variation of raw ingredients (*e.g.*, inconsistent fiber diameter and fiber strength), processing induced variation of flaw size and distribution and curing induced variation of matrix and interface properties. The model proposed in the current study is able to capture this variability (Fig. 5) and well predicts the average values and standard deviations of tensile properties of SHCC M45 (Table 3). Increased discretization fineness from 1 mm (150 sections) to 0.15 mm (1000 sections) has no significant influence on the simulated results, which suggests 150 sampling sections are sufficient to capture the tensile behavior of SHCC M45 in the current study. This can be attributed to that the crack spacing of SHCC M45 observed from experiments is often larger than 1 mm.

Table 3: Tensile properties of experimental and simulated results

	σ_{fc} (MPa)	σ_{cu} (MPa)	ε (%)	δ (μm)	x (mm)
Exp.	3.6±0.1	4.0±0.5	3.1±1.3	58±18	2.4±1.3
Sim.	3.0±0.1	4.2±0.1	3.3±1.2	65±17	2.0±1.2

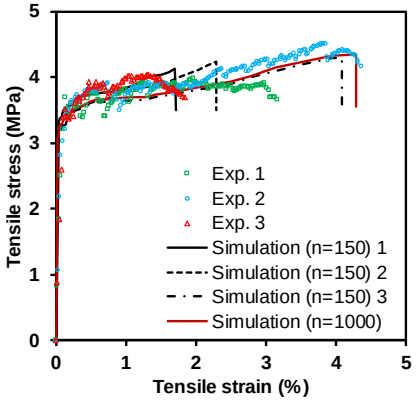

Figure 5: Representative tensile stress-strain curves of SHCC M45 obtained from experiments and numerical simulations

Crack patterns of the experimental specimens alongside with the simulated ones are shown in Fig. 6. As can be seen, the simulation results can clearly capture the variability of the crack spacing with acceptable accuracy. Crack interaction (*i.e.*, crack branching and connecting to adjacent cracks) was observed in experiments for specimens with saturated multiple cracking (*e.g.*, exp. 3), which was not considered in the current numerical simulations.

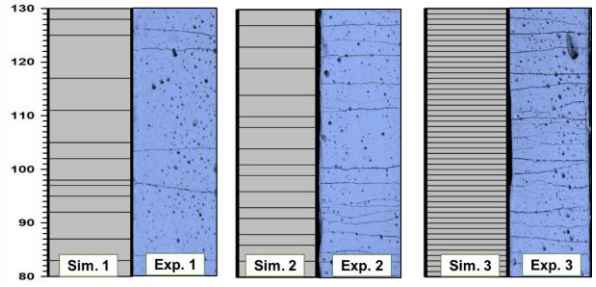

Figure 6: Crack pattern of the representative SHCC M45 specimens obtained from experiments and numerical simulations

In addition, the resulting crack width distribution from the 10 simulated specimens can be obtained at the final failure and shown in Fig. 7. It is fitted as a lognormal distribution with the average crack width of 65 μm, which is slightly higher than the experimental result of 58 μm. The crack width distribution of SHCCs was experimentally observed and reported by Wu and Li [30], in which the histogram of the experimental data is comparable with the simulated results as Fig. 6a. The lognormal distribution of crack width was also experimentally observed in [31]. The variability of crack spacing can be explicitly observed in Fig. 6, and the crack spacing distribution at the final failure for ten simulated specimens is shown in Fig. 6b. It is fitted with a Weibull distribution for SHCC M45, and the average crack spacing was 2.0 mm, which slightly smaller than the experimental measurement of 2.4 mm as Table 3.

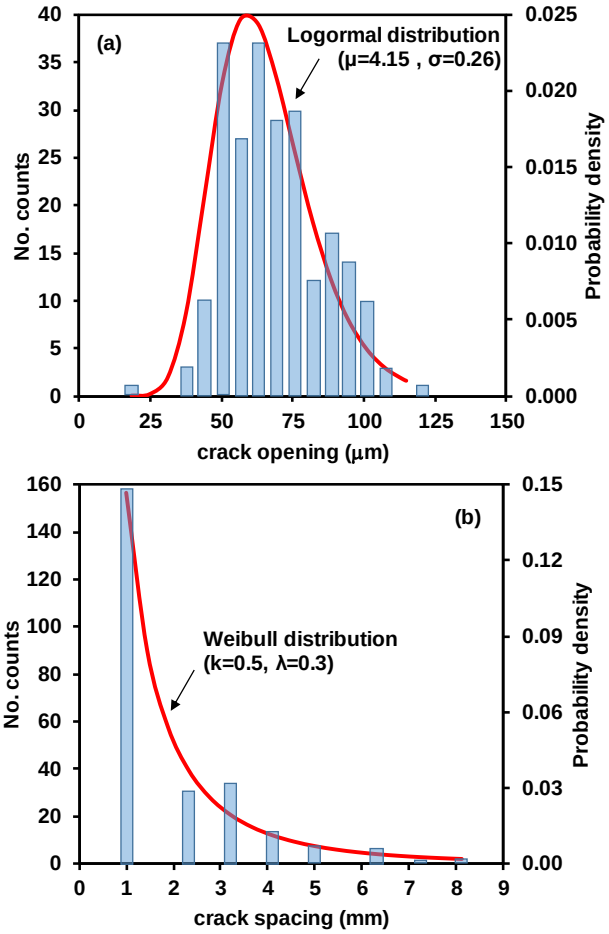

Figure 7: Simulated (a) crack width distribution, and (b) crack spacing distribution of SHCC M45

5 PARAMETRIC STUDIES

Using the proposed model, parametric studies have been conducted to assess the effect of each micro-mechanical parameters on the strain capacity. 20 simulated direct tensile tests are carried out. The micromechanical parameter investigated is treated as a random variable with 10% variation (*i.e.*, taking the

average value with STD of 10% in Table 2) while all other micromechanical parameters are kept as constant (*i.e.*, taking average values with STD of 0% in Table 2). For each simulated test, Monte Carlo simulation is used to generate the value of that specific micromechanical parameter in each crack plane according to the given statistical distribution of the micromechanical parameter along the loading direction. The micromechanical parameters in each cracking plane are then used as inputs to calculate the strain capacity under direct. Fig. 8 shows the stress-strain curves with the minimum and maximum strain capacity resulting from different micro-mechanical parameters.

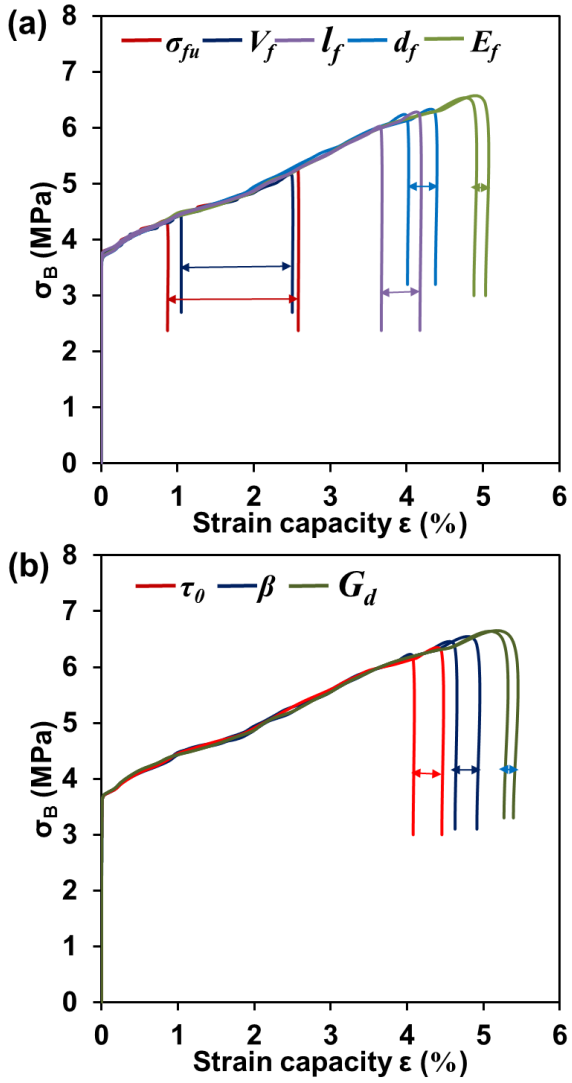

Figure 8: Stress-strain curves resulting from different micro-mechanical parameters in terms of (a) fiber properties; (b) interface properties

Apparently as Fig. 8a, σ_{fu} and V_f are significantly reduced the strain capacity and have larger variation range of strain capacity, compared with l_f, d_f and E_f. The strain capacity of SHCCs are dominated by both the crack width and the cracks number. It was found that significant reduction of the cracks number was caused by σ_{fu} and V_f, resulting in the significant reduction of the strain capacity. In terms of interface properties, τ_0 is the most critical parameter to affect the strain capacity and is often used to tailor the mix design [32].

5 CONCLUSIONS

A micromechanics-based stochastic model of SHCCs is proposed to capture the variability of multiple cracking and tensile behavior by treating fiber, matrix, and fiber/matrix interface properties as random variables and by considering multiple cracking sequence and strain-hardening criteria. This proposed model seems to be a virtual experiments instead of the direct tensile test for given mix design, outputting the tensile stress-strain curves, the multiple cracking sequence and crack pattern, the crack spacing distribution, and the crack width distribution of SHCCs. It is validated by comparing the simulated results with experimental results of a typical SHCC mix. Based on the proposed model, parametric studies indicate that fiber strength σ_{fu}, fiber volume V_f and the interface frictional bond τ_0 are the most critical parameters dominating the tensile strain capacity of SHCCs.

REFERENCES

[1] V. Mechtcherine, Towards a durability framework for structural elements and structures made of or strengthened with high-performance fibre-reinforced composites, Constr. Build. Mater., 31 (2012) 94-104.
[2] G.P.A.G. van Zijl, F.H. Wittmann, B.H. Oh, P. Kabele, R.D. Toledo Filho, E.M.R. Fairbairn, V. Slowik, A. Ogawa, H. Hoshiro, V. Mechtcherine, F. Altmann, M.D. Lepech, Durability of strain-hardening cement-based composites (SHCC), Mater. Struct., 45 (2012) 1447-1463.
[3] V.C. Li, On engineered cementitious

composites (ECC): a review of the material and its applications, J. Adv. Concr. Technol., 1 (2003) 215-230.
[4] V.C. Li, S.X. Wang, Microstructure variability and macroscopic composite properties of high performance fiber reinforced cementitious composites, Probabilistic Engineering Mechanics, 21 (2006) 201-206.
[5] J. Vorel, W.P. Boshoff, Numerical modelling of engineered cement-based composites, 18th International Conference in Engineering MechanicsSvatka, Czech Republic, 2012, pp. 1555-1564.
[6] W.P. Boshoff, G.P.A.G. van Zijl, Time-dependent response of ECC: characterisation of creep and rate dependence, Cem. Concr. Res., 37 (2007) 725-734.
[7] P. Kabele, Stochastic finite element modeling of multiple cracking in fiber reinforced cementitious composites, Fract. Damage of Adv. FRC, (2010) 155-163.
[8] E. Schlangen, Z. Qian, 3D modeling of fracture in cement-based materials, J. Multiscale Model., 1 (2009) 245-261.
[9] M. Luković, H. Dong, B. Šavija, E. Schlangen, G. Ye, K.v. Breugel, Tailoring strain-hardening cementitious composite repair systems through numerical experimentation, Cem. Concr. Compos., 53 (2014) 200-213.
[10] J. Bolander Jr, S. Saito, Discrete modeling of short-fiber reinforcement in cementitious composites, Adv. Cem. Based Mater., 6 (1997) 76-86.
[11] P. Kabele, Multiscale framework for modeling of fracture in high performance fiber reinforced cementitious composites, Eng. Fract. Mech., 74 (2007) 194-209.
[12] P. Kabele, New developments in analytical modeling of mechanical behavior of ECC, J. Adv. Concr. Technol., 1 (2003) 253-264.
[13] V.C. Li, C.K.Y. Leung, Steady-state and multiple cracking of short random fiber composites, J. Eng. Mech., 118 (1992) 2246-2264.
[14] Z. Lin, T. Kanda, V.C. Li, On interface property characterization and performance of fiber-reinforced cementitious composites, Concr. Sci. Eng., 1 (1999) 173-184.
[15] T. Huang, Y.X. Zhang, C. Yang, Multiscale modelling of multiple-cracking tensile fracture behaviour of engineered cementitious composites, Eng. Fract. Mech., 160 (2016) 52-66.
[16] J.X. Li, E.-H. Yang, Probabilistic-based assessment for tensile strain-hardening potential of fiber-reinforced cementitious composites, Cem. Concr. Compos., 91 (2018) 108-117.
[17] C. Lu, C.K.Y. Leung, A new model for the cracking process and tensile ductility of strain hardening cementitious composites (SHCC), Cem. Concr. Res., 79 (2016) 353-365.
[18] P. Kabele, M. Stemberk, Stochastic model of multiple cracking process in fiber reinforced cementitious composites, Proceedings of the 11th International Conference on Fracture, CD ROM, Citeseer, Turin, Italy, 2005.
[19] E.-H. Yang, V.C. Li, Strain-hardening fiber cement optimization and component tailoring by means of a micromechanical model, Constr. Build. Mater., (2010) 130-139.
[20] D.B. Marshall, B.N. Cox, A J-integral method for calculating steady-state matrix cracking stresses in composites, Mech. of Mat., 7 (1988) 127.
[21] A.E. Naaman, G.C. Namur, J.N. Alwan, H.S. Najm, Fiber pull-out and bond slip. I: analytical study, J. Struct. Eng., 117 (1991) 2769.
[22] C.K. Leung, V.C. Li, First-cracking strength of short fiber-reinforced ceramics, Ceramics Engineering Science Proceedings, 1989, pp. 1164-1178.
[23] A.G. Evans, The mechanical performance of fiber-reinforced ceramic matrix composites, Mater. Sci. Eng. A, 107 (1989) 227-239.
[24] T. Kanda, V.C. Li, Multiple cracking sequence and saturation in fiber reinforced cementitious composites, Concr. Res, Technol., 9 (1998) 19-33.
[25] E.-H. Yang, S. Wang, Y. Yang, V.C. Li, Fiber-bridging constitutive law of engineered cementitious composites, J. Adv. Concr. Technol., 6 (2008) 181-193.
[26] S.X. Wang, V.C. Li, Engineered cementitious composites with high volumn fly ash, ACI Mater. J., 104 (2007) 233-241.
[27] E.-H. Yang, Designing added functions in

engineered cementitious composites, The University of Michigan, 2008.
[28] V.C. Li, Y. Wang, S. Backer, Effect of inclining angle, bundling and surface treatment on synthetic fibre pull-out from a cement matrix, Composites, 21 (1990) 132-140.
[29] A. Manor, R.B. Clough, In-situ determination of fiber strength and segment length in composites by means of acoustic emission, Compos. Sci. Technol., 45 (1992) 73-81.
[30] H.-C. Wu, V.C. Li, Stochastic process of multiple cracking in discontinuous random fiber reinforced brittle matrix composites, Int. J. Damage Mech., 4 (1995) 83-102.
[31] H. Liu, Q. Zhang, C. Gu, H. Su, V.C. Li, Influence of micro-cracking on the permeability of engineered cementitious composites, Cem. Concr. Compos., 72 (2016) 104-113.
[32] S. He, J. Qiu, J. Li, E.-H. Yang, Strain hardening ultra-high performance concrete (SHUHPC) incorporating CNF-coated polyethylene fibers, Cem. Concr. Res., 98 (2017) 50-60.